Materials Physics and Mechanics. 2023;51(4): 11-22
Research article
http://dx.doi.org/10.18149/MPM.5142023_2

Submitted: November 3, 2022
Approved: November 14, 2022
Accepted: March 22, 2023

Tribological and tensile behaviour of Si_3N_4 reinforced Cu-Sn matrix composites

B. Adaveesh [1], G.V. Prabhushankar [1], M. Nagaral [2] ✉

[1] Department of Industrial Engineering and Management, Siddaganga Institute of Technology, Tumkur, Karnataka, India

[2] Aircraft Research and Design centre, Hindustan Aeronautics Limited, Bangalore, Karnataka, India

✉ madev.nagaral@gmail.com

Abstract. In the present research, Cu-Sn alloy with 7.5 wt. % of Si_3N_4 particles reinforced composites were fabricated by using conventional stir casting method. As-cast Cu-8 %Sn alloy and Cu-8 %Sn alloy with 7.5 wt. % of Si_3N_4 reinforced composites were evaluated for microstructural studies using SEM and EDS, density, tensile properties and wear behaviour as per ASTM method. Cu-Sn alloy with 7.5 wt. % of silicon nitride particles reinforced composites shown lesser densities as compared to the base Cu-Sn alloy. Further, these composites were exhibited superior tensile strength with slight reduction in the ductility. Pin on disc wear apparatus was used to conduct the wear tests at varying loads and speeds. The wear resistance of Cu-Sn alloy increased with the incorporation of Si_3N_4 particles. Further, applied load and speeds were impacted in the wear behaviour of Cu-Sn alloy composites. As load and speed increased, there was more material loss in as-cast alloy and its composites. Tensile fractured surfaces indicated various fracture modes in Cu-Sn alloy and composites.
Keywords: Cu-Sn alloy; Si_3N_4; tensile behaviour; wear; fractography

Citation: Adaveesh B, Prabhushankar GV, Nagaral M. Tribological and tensile behaviour of Si_3N_4 reinforced Cu-Sn matrix composites. *Materials Physics and Mechanics.* 2023;51(4): 11-22. DOI: 10.18149/MPM.5142023_2.

Introduction

The requirement for lightweight composites with certain features over conventional materials increased as advanced science and technology. This opened the door for additional study into metal matrix composites (MMCs). To enhance the properties of the base metal, materials are reinforced with carbides or organic compounds. MMCs are primarily used in the automotive, aeronautical, and aviation industries [1]. Excellent electrical and thermal, corrosion resistance, and ease of alloying are some highly valuable characteristics of copper. Because of these properties, it is a promising option for most electrical and thermal applications [2]. On the other hand, its subpar mechanical performance prevents its use in many applications. However, this problem can be overcome by incorporating hard ceramic particles like carbides, borides, oxides, and nitrides. These elements increase strength and hardness at the cost of a negligible reduction in electrical conductivity [3].

Many studies illustrate the addition of reinforcements like carbon nanotube, graphite, fly-ash, rice-husk ash, Al_2O_3, Cr_2O_3, TiO_2, TiC, B_4C, SiC, etc., can increase the mechanical properties of copper matrix [4–6]. With high thermal conductivity and less thermal expansion coefficient, Si_3N_4 (silicon nitride) has drawn significant attention because of its superior wear, corrosion thermal shock resistance, and good mechanical properties. Si_3N_4 is an interesting

Publisher: Peter the Great St. Petersburg Polytechnic University

and potential option due to its chemical and mechanical stability at high temperatures for high-temperature applications. Less work is carried out on the effect of Si_3N_4 on copper matrix [7,8].

Several fabrication techniques can produce MMCs, including friction stir, compo-casting; squeeze casting, ultrasonic-assisted casting, spray deposition, powder metallurgy, and diffusion bonding. Stir casting is the most practical and effective for mass production [9,10]. The size, shape, characteristics, proportion, dispersion of the reinforcements, matrix and reinforcement bonding, heat treatment process, and manufacturing method are factors to determine the characteristics of MMC. Decreasing the dislocation motion in the crystal lattice by adding nanoscale reinforcements to the matrix helps to avoid wear [11,12]. It was observed that adding MoS_2 reinforcements to the Al-Si10Mg successfully reduced wear by approximately 65 % [13]. Graphite particles were added as reinforcement to the aluminum alloy to improve its tribological characteristics. These MMCs are capable of self-healing and self-lubrication [14,15]. When sliding distance and velocity increased, the wear rate and specific wear of epoxy/cenosphere syntactic foams dropped, according to a study [16]. According to a study, 5 %, Al_2O_3 added as one of the reinforcements that can improve the composite's wear properties [17]. The composite's hardness and tensile strength are enhanced by enhancing the weight percentage of reinforcement [18].

Machine parts with copper alloy are used where the part experiences significant friction, for example, bearings. Cu-Sn alloys employed in bearings need grease as lubricants, which is more eco-friendly than copper-lead alloys, which constantly use at high temperatures and cause damaging gas releases [19]. Bearings are desired for their higher thermal conductivity, which dissipates heat through friction, excellent wear resistance, compressive strength, fatigue, tensile, shear, and corrosion resistance, and their capacity to handle shocks and vibrations. Higher compressive and tensile strengths boost the bearing material's capacity to withstand the development of cracks and spreading under higher contact pressures and to stop extrusion or other long-term deformation of the bearing [20].

Therefore, this work makes an effort to develop Cu-Sn alloy with 7.5 wt. % of Si_3N_4 particles reinforced composites using stir cast method. Thus prepared composites were evaluated for density, tensile and wear behaviour as per ASTM standards.

Experimental Details

Materials used and composites preparation. In the market today, copper-tin, copper-zinc, and copper-aluminum alloys are the most common bearing materials available. Wear performance is crucial in some applications, especially when exposed to higher loads. Cu-Sn alloys are used in various mechanical and electronic industrial applications because they have outstanding characteristics. Alloys rich in Sn are lead-free solder materials, whereas alloys with rich Cu are used as structural materials. Due to safety and environmental concerns, researchers have become interested in the later application because it eliminates lead toxicity [21].

For the preparation of the composite, a commercially available Cu-Sn alloy was considered. Table 1 shows the elemental composition of Cu-Sn alloy.

Table 1. Chemical composition of Cu-Sn alloy.

Element	Weight, %
Sn	7.85
Al	0.47
Si	0.06
Others	0.20
Cu	Balance

In the current investigation, Si_3N_4 particles with a diameter of 25-30 µm were used as reinforcement material to improve the mechanical behaviour of the Cu-Sn alloy. Cu-Sn/Si_3N_4 composites were fabricated using the liquid stir casting process. Figure 1 shows the Si_3N_4 particles used in the present study.

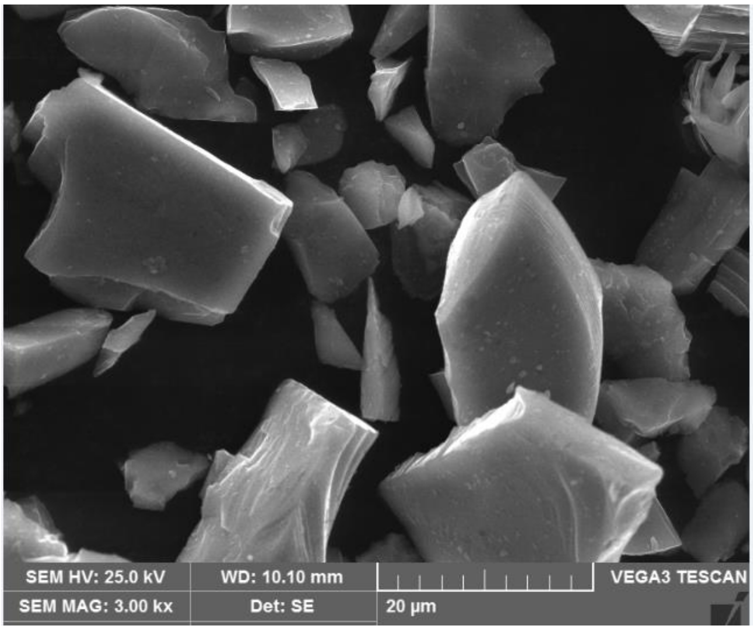

Fig. 1. SEM micrograph of Si_3N_4 particles

The Cu-Sn alloy with micro Si_3N_4 composites was made using a stir process based on the liquid metallurgy method. Metal ingots of a specific amount of Cu 8 % Sn alloy are loaded into an electric furnace and heated until they melt. In this case, the molten metal is heated to a superheated temperature of 1150 °C, whereas the typical melting point of copper tin alloy is 1070 °C. The melting point and the superheated temperature are measured and recorded using thermocouples selected for their accuracy over the relevant temperature range. For about three minutes, solid hexachloroethane (C_2Cl_6) [22] is used to degas the superheated molten metal in the crucible. The molten metal is stirred by a rotor with steel blades, mounted on a shaft and coated with zirconium ceramic. The stirrer is submerged to a depth of about 60 % within the crucible, and the molten metal is agitated to the point of vortex creation by rotating the stirrer at a speed of about 300 rpm. While the molten metal is being stirred, a separate heater is used to heat micro silicon nitride particulates to temperatures of up to 500 °C; these are then slowly poured into the molten metal vortex in stages, amounting to 7.5 % by weight of charged copper tin alloy. Interfacial shear strength is established by continuing to stir until the CuSn alloy matrix and Si_3N_4 reinforcement particulates are completely wet. In order to create Cu-Sn and 7.5 wt. % of Si_3N_4 composites, the molten metal mixture of CuSn alloy matrix and Si_3N_4 composites were poured into the cast iron moulds. Figure 2 shows the Cu-Sn alloy with 7.5 wt. % of Si_3N_4 composites after casting.

Fig. 2. Cu-Sn alloy and Si_3N_4 composite

Testing of prepared composites. Cu-Sn base alloy and Cu-Sn 7.5 wt. % Si_3N_4 composites were used for the microstructural study. Using a 200–320 grit size abrasive paper, the specimen's surface was initially made flat, and then finer lines were added by using 600–1200 grit size. Using Keller's reagent for an etching process, the last layer is removed chemically, and an SEM is employed to inspect it.

The displacement method and density measurements per ASTM D792-66 were used to determine measured density values, and the rule of mixture was utilized to calculate theoretical density. The specimen is initially submerged in a known volume of distilled water. Physical, digital balance equipment calculates the specimen's mass after it has been immersed in water. After the sample is submerged, the volume is determined by the amount of displaced water. The mass and volume data were collected for both copper-tin alloy and copper-tin alloy with 7.5 wt. % of Si_3N_4 composites. Then theoretical and experimental densities were compared.

Tensile tests were conducted on the composites to look into their mechanical properties. Round test specimens made of Cu-Sn base alloy and Cu-Sn with 7.5 wt. % of Si_3N_4 composites are employed for tensile testing based on standard ASTM-E8 at room temperature using a computerized UTM with a 400 kN capacity. Three samples were used to compute yield strength, UTS (ultimate tensile strength), and elongation %, three samples were taken and calculated average value for results. Figure 3 shows the schematic diagram of tensile test specimen and machined tensile test specimen as per standard respectively.

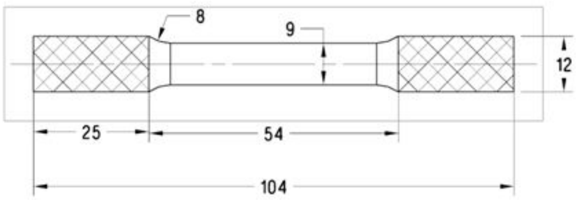

(a)


(b)

Fig. 3. Schematic diagram of tensile test specimen (a) and machined tensile test specimen (b)

Wear is removing material from one or more solid surfaces that are in friction. The standard wear test estimates the amount of material removed under specific circumstances. A wear test was performed on numerous specimens using pin-on-disc equipment. The samples hold the counter head of a revolving circular disc firmly with a 120 mm circumference wear track by a pin holder. Dead weights were put to the pin on the other side of the circular disc to calculate the wear.

Fig. 4. Wear test specimen

The specimens are fabricated based on standard ASTM-G99, and the disc is cleaned using acetone. Samples prepared for the wear test collect information about wear from electronic sensors. The pin's surface was initially flawed. The rotating disc is meticulously cleaned to provide precise readings. The next step is to fix the samples to the chuck. The track has a diameter of 120 mm. Figure 4 shows the samples that were used in the wear test, having 8 mm in diameter and 30 mm length. Wear test were carried out at varying loads and speeds. Varying loads of 1 to 3 Kg at 300 rpm and varying speeds of 100 to 300 rpm at 3 Kg load at 2500 m sliding distance were used.

Results and Discussion

Microstructural study. The microstructural characterizations of specimens are examined by SEM with EDS attachment. Figure 5 demonstrates the SEM micrographs of Cu-Sn alloy and micro Si_3N_4 reinforced composites. Figure 5(a) shows the SEM of CuSn alloy. Figure 5(b) shows the SEM images of Cu-Sn alloy with 7.5 wt.% of Si_3N_4 reinforced composites. It confirms that most of micro Si_3N_4 particles are mixed uniformly in Cu-Sn alloy. Further, these figures disclose the uniformity of the prepared composites.

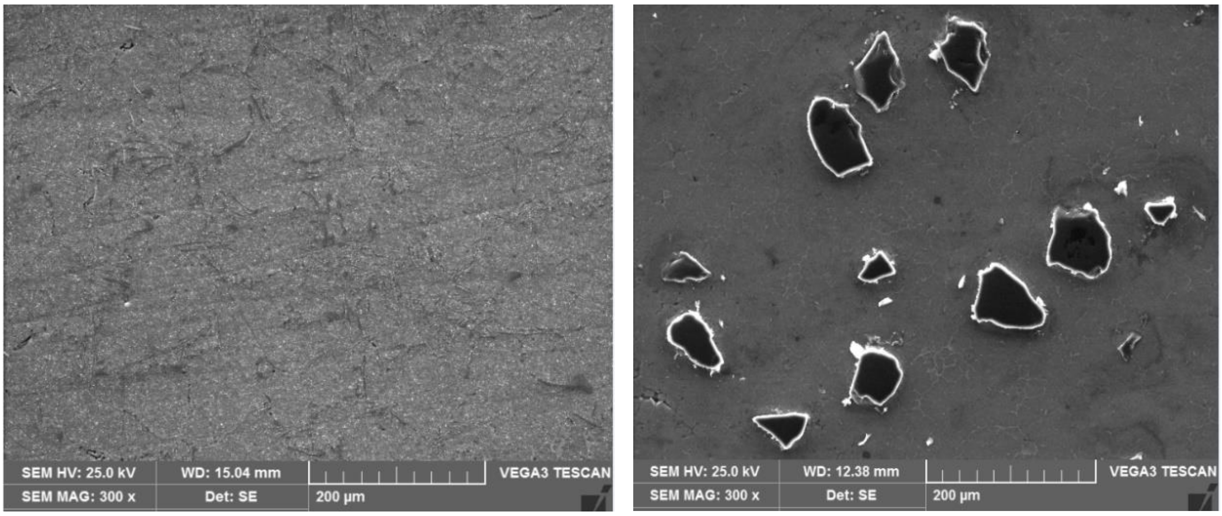

(a) (b)

(a) (b)

Fig. 5. SEM micrographs of (a) As-cast Cu-Sn alloy (b) Cu-Sn alloy with 7.5 wt. % of Si_3N_4 composites

As can be seen in Fig. 5(b), micro Si_3N_4 reinforcement particles are evenly dispersed throughout the CuSn matrix, as revealed by scanning electron micrographs. This also shows that there are no cracks, holes, or pores present. Micro Si_3N_4 reinforcement particles and the 'CuSn alloy matrix are observed to form strong interfacial bonds. From the above SEM images, it is clear that the CuSn with micro Si_3N_4 particulate composite is extremely strong and has a significant impact on both mechanical and tribological properties due to the uniform distribution of reinforcement particles, the lack of defects in the casting process, and the good interfacial bonding between the different materials.

Element detection by spectroscopy (EDS) is a powerful and useful technique for identifying elements and their relative abundance. While chemical analysis can identify which elements are present in a given sample, a more precise measure of their relative abundance requires EDS. Compositions of the aforementioned composites are shown in Fig. 6, and EDS is used for elemental analysis of both Cu-Sn alloy and Cu-Sn with Si_3N_4 reinforcement (Fig. 6(a,b)).

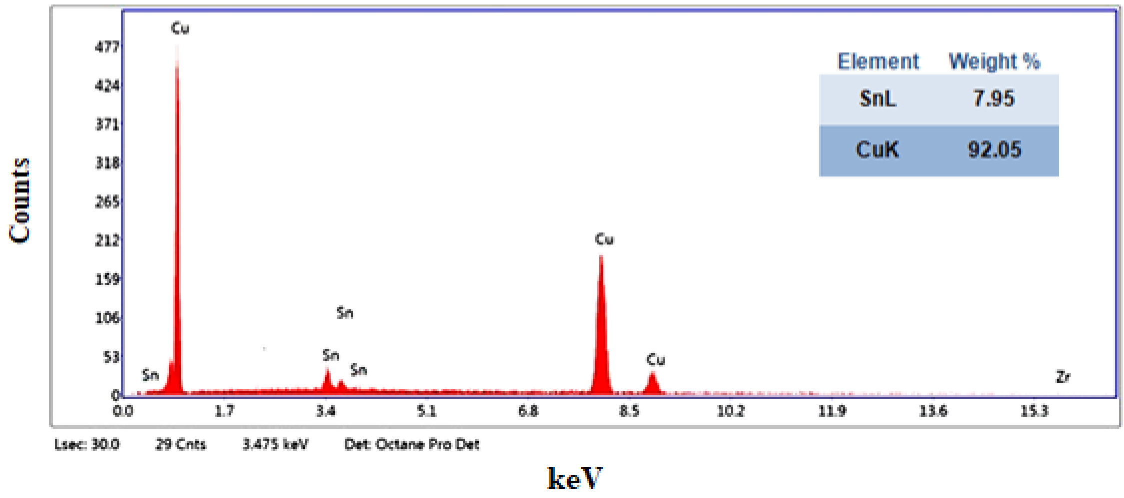

(a)

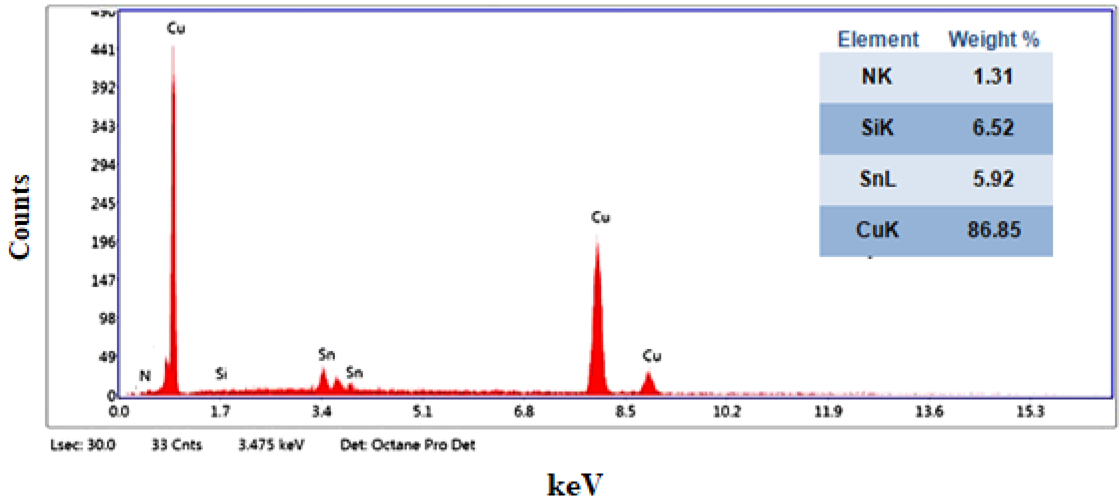

(b)

Fig. 6. EDS spectrums of (a) As-cast Cu-Sn alloy (b) Cu-Sn alloy with 7.5 wt.% of Si_3N_4 composites

As can be seen from the preceding graphs, the Y axis represents the number of occurrences and the X axis represents the intensity of those occurrences. The EDS spectrograph of as cast Cu-Sn alloy is shown in Fig. 6(a). Copper is the most abundant element in the sample, with tin as an alloying element also confirmed by the spectrum. The presence of silicon nitride is confirmed with Si and N peaks in the EDS spectrum of Cu-Sn alloy with 7.5 wt.% of Si_3N_4 particles composites, shown in Fig. 6(b).

Density measurements. Explanations of the theoretical and experimental values obtained for various samples are provided in Fig. 7. In this study, it is expected that experimental values will be similar to the calculated theoretical values. Since theoretical values are calculated using standardised formulas, it is extremely unlikely that the experimental values will match exactly.

Figure 7 displays a comparison between the theoretical and experimental densities of an as cast Cu-Sn alloy and a Cu-Sn alloy reinforced with 7.5 wt. % of Si_3N_4 composites. The density of Si_3N_4 is only 3.17 g/cm^3, while the density of Cu-Sn alloy is 8.80 g/cm^3. Since Si_3N_4 has a lower density than CuSn alloy, adding 7.5 wt. % of Si_3N_4 to the alloy results in a lower composite density of 7.765 g/cm$_3$. Furthermore, the difference between the theoretical and experimental densities can be seen to be smaller than expected. When Si_3N_4 is added, density drops, which is consistent with the findings of other researchers [23]. The closeness of the experimental densities to the theoretical densities, as shown in Fig. 7, is further evidence of the high quality of the specimens prepared.

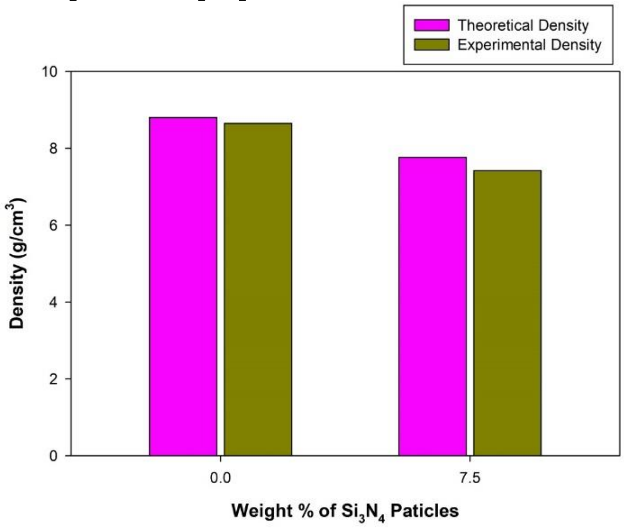

Fig. 7. Theoretical and experimental densities of Cu-Sn alloy and its Si_3N_4 reinforced composites

Tensile behaviour. The analysis of the tensile behaviour of base metal Cu-Sn and Cu-Sn 7.5 wt. % Si_3N_4 composites are shown in Figs. 8–10. These properties include UTS, yield strength, and percentage of elongation.

Figures 8 and 9 represent the ultimate and yield tensile strength of Cu-Sn alloy and Cu-Sn alloy with 7.5 wt. % of Si_3N_4 composites. Cu-Sn 7.5 wt. % Si_3N_4 composites demonstrated a 32.941 % increase in UTS, a 28.865 % rise in YS, and a 23.002 % decrease in elongation percentage when compared to Cu-Sn base metal. It is clear from Figs. 8 and 9 that Si_3N_4 particles significantly increase the tensile strength of the Cu-Sn matrix. Dislocations occur through the matrix due to the application of a uniaxial tensile load. Plastic zones are created when they aggregate close to the reinforcement particle boundary. The difference in the thermal expansion coefficient between the matrix and the reinforcement phase determines the size of this plastic zone. The copper matrix-reinforcement interface acts as an effective barrier against the spread of dislocations across the interface. Si_3N_4 hard particles give the matrix strength, and as a result of this process of strengthening, the composite gives greater resistance to tensile force.

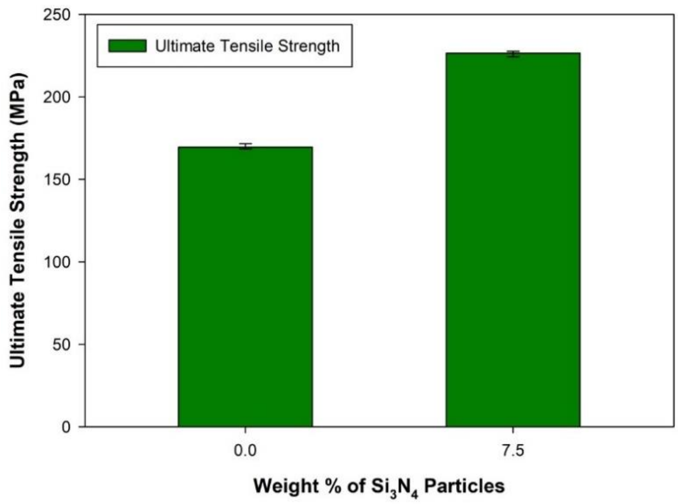

Fig. 8. Ultimate strength of Cu-Sn alloy with Si_3N_4 composites

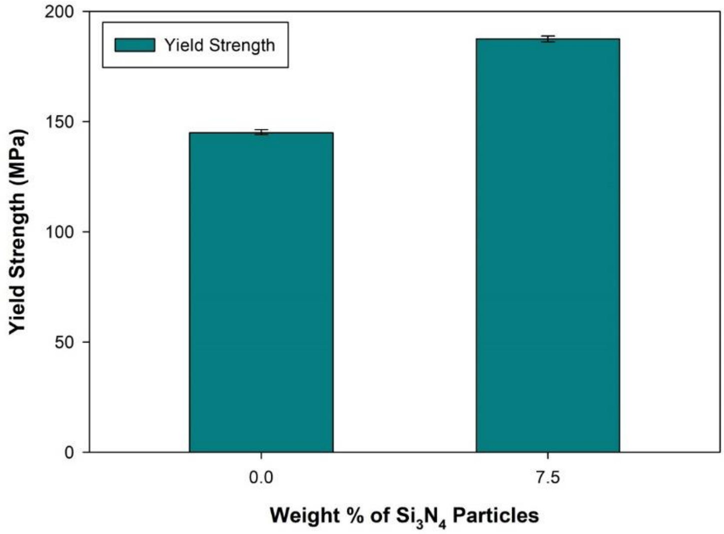

Fig. 9. Yield strength of Cu-Sn alloy with Si_3N_4 composites

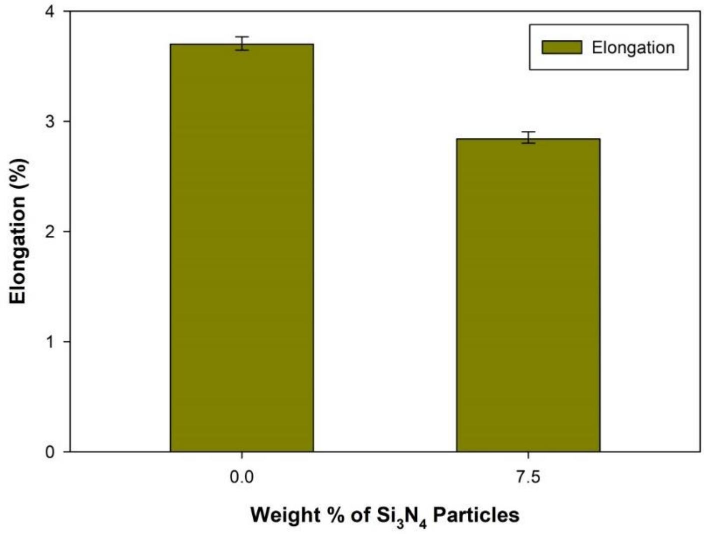

Fig. 10. Elongation of Cu-Sn alloy with Si_3N_4 composites

According to the results of the present study, the hard Si_3N_4 particles are directly responsible for the improvement in yield quality of the composite by delectating the Cu-Sn amalgam system and bringing greater quality obstruction of the composite against the associated pliability load. Miniaturized scale molecule reinforced composites have a redesigned quality because of the uniformly sized, hard fired particles in the lattice that act as an impediment to the plastic flow.

Micro Si_3N_4 particles' influence on Cu-Sn alloy and composites' ductility is depicted in Fig. 10. When an axial load is applied to a specimen, the material stretches to accommodate the stress. The elongation of a tensile test specimen is calculated by dividing the gauge length it has at failure by the original gauge length. When describing the ductility of a material, the elongation of a specimen is typically expressed as a percentage and is greater the more the material can be stretched. Tensile testing results for as cast Cu-Sn alloy and Cu-Sn alloy reinforced with 7.5 wt. % Si_3N_4 particulates are shown in Fig. 10. When Si_3N_4 particles are added to as-cast Cu-Sn alloy, the elongation percentage drops.

Fractography. This study analyses the materials fractured surface. Figure 11 depicts the SEM of the tensile fractured samples of base metal Cu-Sn and Cu-Sn 7.5 wt. % Si_3N_4 composites. Figure 11(a) shows the ductile fracture of the Cu-Sn base metal. In SEM image, wrinkles are observed on the surface. Initially voids are observed, and these are developed because of plasticity, and at last cracks are observed that cause the material to ductile fracture. Figure 11(b) shows the cracked surface images of Cu-Sn 7.5 wt. % Si_3N_4 composites in comparison to its matrix, with more minor wrinkles visible. This demonstrates that the Cu-Sn 7.5 wt. % Si_3N_4 composites have brittle fracture behaviour. The SEM images reveal large voids and crack propagation. The strong reinforcing particles trapped in the matrix material are essential in slowing the spread of cracks in the materials. Therefore, compared to the matrix material, these materials have greater tensile strength.

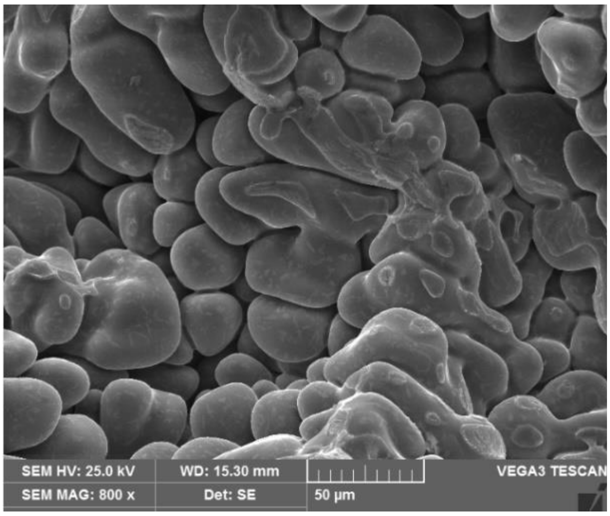

(a)

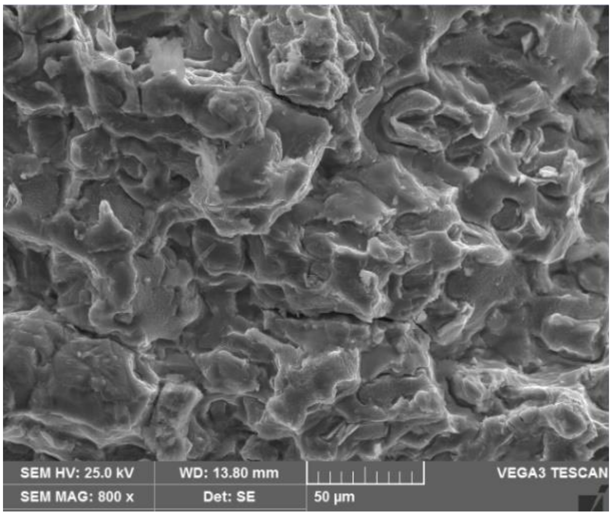

(b)

Fig. 11. Tensile fractured surfaces SEM images (a) as-cast Cu-Sn alloy and (b) Cu-Sn alloy - 7.5 wt. % of Si_3N_4 composites

Wear Properties. Wear tests were performed on the composites that were reinforced with Si_3N_4. Initially, castings are machined according to ASTM-G99 for wear testing. Six specimens were tested with various loads and constant speeds for each composition test, while another six samples were tested with different speeds and constant loads. The results of using pin-on-disc technology under different conditions. Based on this finding, the wear behaviour is examined. Here it is analysed how the loaded speed affects the wear loss.

Influence of Load. The load is a key factor in the wear and tear that occurs. The effect of normal load in wear experiments has been the subject of extensive research in order to better understand the wear rate of copper alloys. Moreover, graphs for wear loss against different loads of 1, 2, and 3 kg at a constant distance of 2500 metres and speed of 300 rpm have been plotted to investigate the impact of load on wear. Load's influence on the wear behaviour of Cu-Sn alloy and Si_3N_4 reinforced composites is depicted in Fig. 12.

When moving the load up from 1 to 3 kg, the graph 12 shows that wear increases for both the composites and the base Cu-Sn alloy. The temperature of the sliding surface and the pin rises above the critical value at a maximum load of 3 kg. Accordingly, wear loss of the matrix Cu-Sn alloy and Cu-Sn alloy with 7.5 wt. % of Si_3N_4 composites increases with the increase in pin load. As shown in Fig. 12, as cast Cu-Sn alloy experiences the greatest wear loss under all loading conditions. We can see that by incorporating reinforcement into the Cu-Sn alloy, the composites' wear loss is reduced. Some research suggests that the high hardness of Si_3N_4 particulates, which acts as a barrier for the wear loss, is responsible for the improved wear resistance of the Cu-Sn alloy with 7.5 wt. % of Si_3N_4 composites. The increased wear misfortune as the load is increased from 1 to 3 kg is mainly due to the increased contact area between the pin and the steel plate. As the area of contact increases during a wear test, more heat is generated, eventually leading to the delamination of the compound or composite.

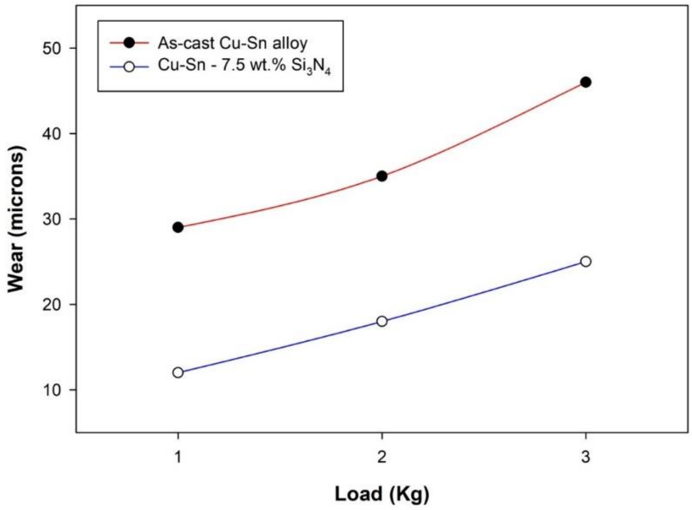

Fig. 12. Effect of load on the wear behaviour of Cu-Sn alloy and its Si_3N_4 composites

Influence of Speed. It is absorbed, that wear loss varies depending on speed. Experiment is conducted with a fixed weight of 3 kg and a variable speed disc revolving at 100, 200, and 300 rpm. It is observed that the sliding speed increases with increase in wear rate, as shown in Fig. 13. Wear loss is more pronounced in base alloys than in composites reinforced with Si_3N_4. All wear loss in Cu-Sn matrix alloy and Si_3N_4 composites is determined by sliding speed. The Cu-Sn matrix alloy and generated composites experience significant wear as the speed is raised from 100 to 300 rpm. Composites degrade at high temperatures; therefore, wear happens as the sliding speed rises.

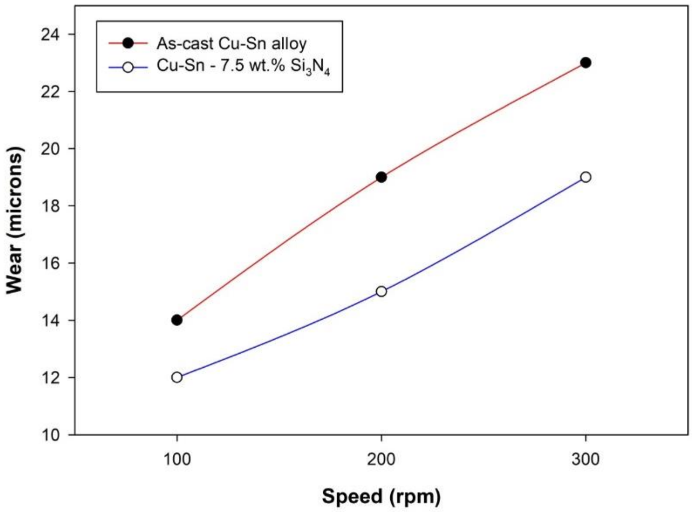

Fig. 13. Effect of speed on the wear behaviour of Cu-Sn alloy and its Si_3N_4 composites

It can be inferred from Fig. 13 that wear misfortune volume increases with velocity. When comparing Si_3N_4-enhanced composites to their base Cu-Sn counterparts, the effect of sliding rate is greater for the latter. The wear loss of the composites is much less than that of the Cu-Sn matrix alloy at all sliding speeds, and it is especially low in the case of the Cu-Sn alloy with 7.5 wt.% of Si_3N_4 composites. Wear losses in the composite are reduced when Si_3N_4 powder is added to the mix. The wear loss of the composites is less than that of the Cu-Sn alloy and the Cu-Sn compound with Si_3N_4 composites at all sliding velocities. Wear problems in the composite are fundamentally alleviated by the addition of Si_3N_4 particles. Additionally, wear loss increases as sliding rate increases due to the expansion of the composite at elevated temperatures caused by scouring activity. Temperature increases brought on by greater sliding rates also lead to plastic deformation of the test specimen. Therefore, increased wear problems are a direct result of widespread delamination.

Conclusions

A stir casting process was used to make Cu-Sn alloy with 7.5 wt. % of Si_3N_4 composites. The prepared composites were studied for microstructural characterization by using SEM and EDS. Scanning electron micrographs were shown the dispersion of Si_3N_4 particles in the Cu-Sn alloy matrix. Further, Si_3N_4 particles in the Cu-Sn alloy matrix were confirmed by the EDS spectrums containing the Si and N elements. With the incorporation of micro sized Si_3N_4 particles, various mechanical properties like, ultimate and yield strengths were improved. Ultimate tensile strength of as-cast Cu-Sn alloy was 170 MPa, with 7.5 wt. % of Si_3N_4 particles it was found 225.96 MPa. Addition of hard nitride particles decreased ductility of Cu-Sn alloy, the lowest ductility was observed in the case of Cu-Sn alloy with 7.5 wt. % of Si_3N_4 particles. Tensile fractured surfaces of as-cast `Cu-Sn alloy indicated the ductile mode of fracture, whereas composites shown brittle fracture. Wear resistance of Cu-Sn alloy improved with the addition of silicon nitride particles. Further, as load and speed increased, wear loss increased in the base Cu-Sn alloy and its composites.

References

1. Sallahauddin A, Nagaral M, Reddappa HN, Auradi V. Effect of B_4C particulates addition on wear properties of Al7025 alloy composites. *American Journal of Materials Science.* 2015;5(3C): 53-57.
2. Matti S, Shivakumar BP, Shashidhar S, Nagaral M. Dry sliding wear behavior of mica, fly ash and red mud particles reinforced Al7075 alloy hybrid metal matrix composites. *Indian Journal of Science and Technology*. 2021;14(4): 310-318.
3. Davis JR. Copper and Copper Alloys. In: *ASM Specialty Handbook*. ASM International; 2001. p.446–448.
4. Rathod S, Modi OP, Prasad BK, Chrysanthou A, Vallauri D, Deshmukh VP. Cast in situ Cu-TiC composites: synthesis by SHS route and characterization. *Materials Science and Engineering A*. 2009;502(1–2): 91–98.
5. Dash K, Chaira D, Ray BC. Microstructural evolution and sliding wear studies of copper-alumina micro and nanocomposites fabricated by spark plasma sintering. *Journal of Mechanical Behaviour of Materials.* 2015;24(1-2): 25–34.
6. Shojaeepour F, Abachi P, Purazrang K, Moghanian AH. Production and properties of Cu/Cr_2O_3 nanocomposites. *Powder Technology*. 2012;222: 80–94.
7. Saravanakumar S, Gopalakrishnan S, Kalaiselvan K. Development of empirical relationships for prediction of mechanical and wear behavior of copper matrix surface composite by friction stir processing technique. *Archives of Metallurgy and Materials*. 2021;66(2): 617–626.
8. Ying DY, Zhang DL. Processing of $Cu\text{-}Al_2O_3$ metal matrix nanocomposite materials by using high energy ball milling. *Materials Science and Engineering A.* 2000;286(1): 152–156.
9. Zhao Y, Fan H. Effect of pulse parameters on the microstructural evolution and properties of jet electrodeposited $Cu–Al_2O_3$ nanocomposite coating. *Materials Transactions.* 2021;62(6): 726–730.

10. Wang F, Li Y, Wang X, Koizumi Y, Kenta Y, Chiba A. In-situ fabrication and characterization of ultrafine structured Cu-TiC composites with high strength and high conductivity by mechanical milling. *Journal of Alloys and Compounds.* 2016;657: 122–132.
11. Sathiskumar R, Murugan N, Dinaharan I, Vijay SJ. Characterization of boron carbide particulate reinforced in situ copper surface composites synthesized using friction stir processing. *Materials Characterization*. 2013;84: 16–27.
12. Zhao N, Li J, Yang X. Influence of the P/M process on the microstructure and properties of WC reinforced copper matrix composite. *Journal of Materials Science.* 2004;39(15): 4829–4834.
13. Vinoth KS, Subramanian R, Dharmalingam S, Anandavel B. Mechanical and tribological characteristics of stir-cast Al-Si10Mg and self-lubricating Al-Si10Mg/MoS_2 composites. *Materials Technology*. 2012;46(5): 497–501.
14. Venkat Prasat S, Subramanian R, Radhika N, Anandavel B. Dry sliding wear and friction studies on AlSi10Mg–fly ash–graphite hybrid metal matrix composites using Taguchi method. *Tribology and Materials Surface Interfaces.* 2011;5(2): 72–81.
15. Rajesh S, Gopala Krishna A, Rama Murty Raju P, Duraiselvam M. Statistical analysis of dry sliding wear behavior of graphite reinforced aluminum MMCs. *Procedia Materials Science.* 2014;6: 1110–1120.
16. Vyasaraj M, Gururaj P, Mrityunjay D, Gaitonde VN, Siddhalingeshwar IG, Kishore VasanthCS, Nikhil. Dry sliding wear of epoxy/cenosphere syntactic foams. *Tribology International.* 2015;92: 425–438.
17. Kanthavel K, Sumesh KR, Saravana Kumar. Study of tribological properties on Al/Al_2O_3/MoS_2 hybrid composite processed by powder metallurgy. *Alexandria Engineering Journal.* 2016;55(1): 13–17.
18. Radhika N, Subramanian R. Effect of reinforcement on wear behavior of aluminum hybrid composites. *Tribology and Materials Surface Interfaces*. 2013;7: 36–41.
19. Kestursatya M, Kim JK, Rohatgi PK. Wear performance of copper–graphite composite and a leaded copper alloy. *Materials Science and Engineering A.* 2003;339(1-2): 150–158.
20. Balakrishnan S, Baker CE, Rahnejat H. Fundamental of hydrodynamic journal bearings: an analytical approach. In: *Tribology and dynamics of engine and powertrain: fundamentals, applications and future trends*. Woodhead Publishing; 2010. p.591–594.
21. Zhai W, Wang WL, Geng DL, Wei B. A DSC analysis of thermodynamic properties and solidification characteristics for binary Cu-Sn alloys. *Acta Materials.* 2012;60(19): 6518–6527.
22. El-Daly AA, Hammad AE, Fawzy A, Nasrallh DA. Microstructure, mechanical properties, and deformation behaviour of Sn–1.0Ag–0.5Cu solder after Ni and Sb additions. *Materials Design.* 2013;43: 40–49.
23. Nagaral M, Deshapande RG, Auradi V, Satish BP, Samuel Dd, Anilkumar MR. Mechanical and wear characterization of ceramic boron carbide-reinforced Al2024 alloy metal composites. *Journal of Bio-and Tribo-Corrosion*. 2021;7(1): 1–12.

THE AUTHORS

B. Adaveesh
e-mail: badaveesh@yahoo.co.in

G.V. Prabhushankar
e-mail: gvpshankar@sit.ac.in

Madeva Nagaral
e-mail: madev.nagaral@gmail.com